Heliyon 9 (2023) e15073

Contents lists available at ScienceDirect

Heliyon

journal homepage: www.cell.com/heliyon

Research article

Proposal of optically tunable and reconfigurable multi-channel bandstop filter using sum-frequency generation in a PPLN waveguide

Yuzhe Sun [a], Zhefeng Hu [a,b,*], Shuting Cheng [a], Yachao Zhao [a], Lingfang Wang [a], Kaixin Chen [a], Wenbao Sun [c]

[a] School of Optoelectronic Science and Engineering, University of Electronic Science and Technology of China, Chengdu, 611731, China
[b] Wuhan National Laboratory for Optoelectronics, Huazhong University of Science and Technology, Wuhan, 430074, China
[c] Tianjin Jinhang Technical Physics Institute, Tianjin, 300308, China

ARTICLE INFO

Keywords:
All-optical
Tunable and reconfigurable filter
Multi-channel
Periodically poled lithium niobate waveguide
Nonlinear optics

ABSTRACT

A multi-wavelength bandstop filter is proposed and numerically demonstrated using the sum-frequency generation (SFG) process in a waveguide of periodically poled lithium niobate (PPLN). This proposed device achieves channels number reconfigurable, central filtering wavelength of each filtering channel independently tunable and extinction ratios (ERs) equalized via all-optical methods.

1. Introduction

In optical communication, it is often necessary to filter the signals. The traditional processing method is to filter the signal in electrical domain after opto-electric conversion. Then the processed signal is modulated onto the optical carrier again by electro-optic conversion. In this way, the opto-electric, electro-optic conversion and signal processing in electrical domain will experience the electronic bottlenecks. Therefore, all-optical filters become the key components in the future all-optical communication networks [1]. Besides the applications in optical communications, all-optical filters also play important roles in the field of microwave photonics [2,3] and optical sensing [4,5]. In many application scenarios, such as wavelength division multiplexing (WDM) network, multi-point sensing et al., devices achieve multi-channel filtering, wavelength tunable and channel number reconfigurable are extremely desired to provide the flexibility of the optical communication systems.

As a synthetic single crystal material, lithium niobate (LN) crystal has attracted great attention in recent years because of the large electro-optical (EO), ferroelectric and nonlinear optical coefficients. These result in its wide use for EO modulation [6–8], electric field sensing [9–11], and all-optical signal processing [12–14]. In previous work, optical filter used for single channel filtering is constructed based on the sum-frequency generation (SFG) effect in a periodically poled LN (PPLN) waveguide. The scheme achieves tunability on central wavelength in a large range [15,16].

In fact, several SFG processes have the potential to proceed simultaneously between multi-pairs of pump and signal lights, if each pair satisfies the frequency condition and the quasi-phase matching (QPM) condition. Based on this idea, we propose and numerically

* Corresponding author. School of Optoelectronic Science and Engineering, University of Electronic Science and Technology of China, Chengdu, 611731, China.
E-mail address: zfhu@uestc.edu.cn (Z. Hu).

https://doi.org/10.1016/j.heliyon.2023.e15073
Received 20 December 2022; Received in revised form 24 March 2023; Accepted 27 March 2023
Available online 6 April 2023

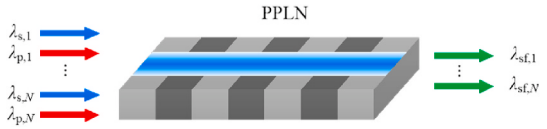

Fig. 1. Structure of the proposed PPLN based multi-channel bandstop filter.

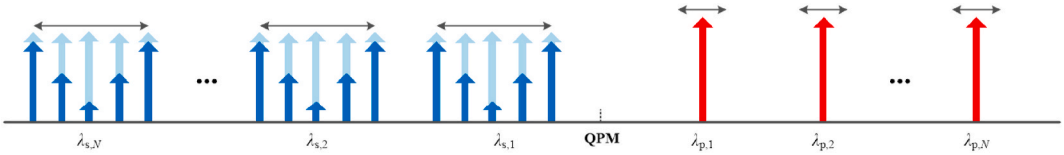

Fig. 2. Working principle of the multi-channel bandstop optical filter.

analyze a multi-wavelength bandstop optical filter employing multi-channel SFG processes in a PPLN waveguide in the present paper. The central wavelength and extinction ratio (ER) of each filtering channel can be tuned independently. The number of these bandstop channels can be reconfigured. After adjusting the power values of pump lights coupled into the waveguide, ER equalization is achieved in all the channels.

2. Basic theory

Fig. 1 illustrates the structure of proposed PPLN based multi-channel bandstop filter using SFG processes. N pairs of signal and pump lights are coupled into this filter together. m-th pair of signal and pump lights are consumed and produce sum-frequency light, through m-th SFG process.

$$\omega_{s,m} + \omega_{p,m} = \omega_{sf,m} \tag{1}$$

$$\Delta k_m = k_{sf,m} - k_{s,m} - k_{p,m} - \frac{2\pi}{\Lambda} = 0 \tag{2}$$

Here, $\omega_{s,m}$, $\omega_{p,m}$ and $\omega_{sf,m}$ ($m = 1, 2, \ldots N$) are the angular frequencies of the signal, pump and sum-frequency lights and $k_{s,m}$, $k_{p,m}$ and $k_{sf,m}$ are the propagation constants of the three lights of m-th SFG process, respectively. Thus, Δk_m represents the phase mismatching. Λ is the poling period of the PPLN waveguide.

When the frequency condition of Eq. (1) and the phase-matching condition of Eq. (2) are strictly satisfied, the phase mismatching is totally compensated. Thus, the energy of the signal light is depleted most. However, when the wavelength of signal light deviates from above QPM condition, the phase mismatching increases seriously. Therefore, this signal light is hardly consumed. In this way, Fig. 2 illustrates a bandstop filtering channel is achieved on each signal transmission spectrum. If we tune the input pump wavelength of a channel, the central wavelength of the filtering channel will change accordingly. The tolerance of optical wavelength deviation is very small, therefore the input lights in different pairs cannot meet the QPM condition. This results in that each SFG process is independent, so the adjusting of the central wavelength of each filtering channel will not influence other channels. The number of these bandstop channels is also reconfigured by changing pump lights number coupled into the waveguide.

The interaction among three light fields in m-th filtering channel can be described by following nonlinear coupled wave equations.

$$\begin{aligned}
\frac{dA_{s,m}}{dz} &= i\omega_{s,m}\kappa_m A^*_{p,m} A_{sf,m} \exp(i\Delta k_m z) \\
\frac{dA_{p,m}}{dz} &= i\omega_{p,m}\kappa_m A^*_{s,m} A_{s,m} \exp(i\Delta k_m z) \\
\frac{dA_{sf,m}}{dz} &= i\omega_{sf,m}\kappa_m A_{p,m} A_{s,m} \exp(-i\Delta k_m z)
\end{aligned} \tag{3}$$

where $A_{s,m}$, $A_{p,m}$ and $A_{sf,m}$ are the slowly varying envelope of the signal, pump and sum-frequency lights of m-th channel, respectively. κ_m is the nonlinear coupling coefficient of the m-th SFG process. It can be given as

$$\kappa_m = \frac{2d_{33}}{\pi}\sqrt{\frac{2\mu_0}{c n_{s,m} n_{p,m} n_{sf,m} A_{eff}}} \tag{4}$$

Here, $n_{s,m}$, $n_{p,m}$ and $n_{sf,m}$ are the refractive indices of the signal, pump and sum-frequency lights of m-th channel, respectively. c and μ_0 are light velocity and permeability of vacuum, respectively. A_{eff} is the effective reaction area.

The signal conversion efficiency in the m-th channel is expressed as follows

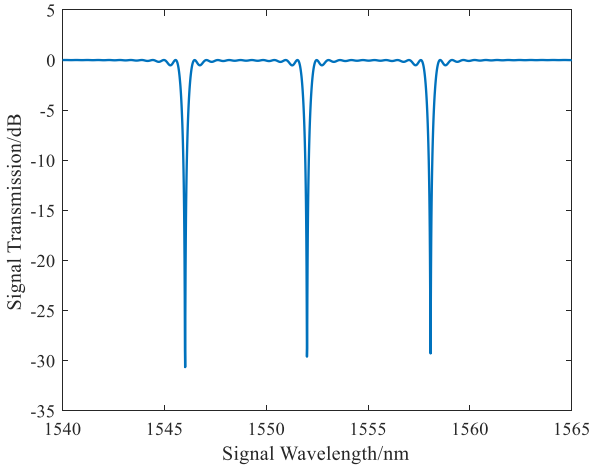

Fig. 3. The output signal transmission spectrum of the three-channel filter.

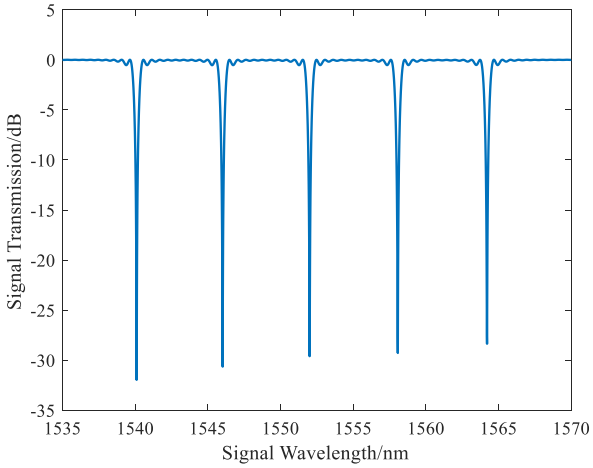

Fig. 4. The output signal transmission spectrum of the five-channel filter.

$$\eta_m = \frac{\left|A_{s,m}(0)\right|^2 - \left|A_{s,m}(L)\right|^2}{\left|A_{s,m}(0)\right|^2} \times 100\% \tag{5}$$

where $A_{s,m}(z)$ represents that signal amplitude of m-th channel is a function of transmission distance z, which can be solved by Eqs. (3) and (4). L is the length of the PPLN waveguide.

3. Simulated calculation and discussion

In the following simulations, the proposed filter structure is based on lithium niobate bulk material. We suppose the poling period Λ is 19.08 μm at 25 °C. The corresponding second-harmonic generation (SHG) wavelength is 1550 nm. The length of the PPLN is 50 mm.

In the beginning, the filter is numerically analyzed with three filtering channels. The wavelengths of three pumps coupled into the waveguide are chosen at 1542 nm, 1548 nm and 1554 nm. The output signal transmission spectrum is plotted in Fig. 3. Here, the three pump powers are all set as 65 mW. The corresponding signal powers are all set as 1 mW. Three bandstop filtering channels are observed at 1558 nm, 1552 nm and 1546 nm in the output signal transmission spectrum, respectively. Actually, the wavelength of signal meeting the QPM condition of Eqs. (1) and (2) with the input pump wavelength in each filtering channel is just the central wavelength of the bandstop filtering channel. The ERs of the three filtering channels are 29.28 dB, 29.60 dB and 30.65 dB, respectively. According to Eq. (5), the corresponding signal conversion efficiencies are 99.88%, 99.89% and 99.91%, respectively. The bandwidths of them are all 0.43 nm. The bandwidths of different channels are much closed. As discussed in single channel filter, the bandwidth changed very little following the filtering wavelength [16].

In the next step, two new pump lights with wavelengths at 1536 nm and 1560 nm are added at the input port. Consequently, two

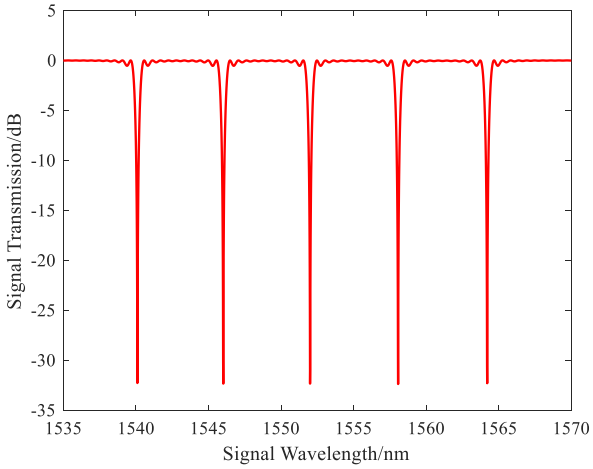

Fig. 5. The ERs equalized output signal transmission spectrum of the five-channel filter.

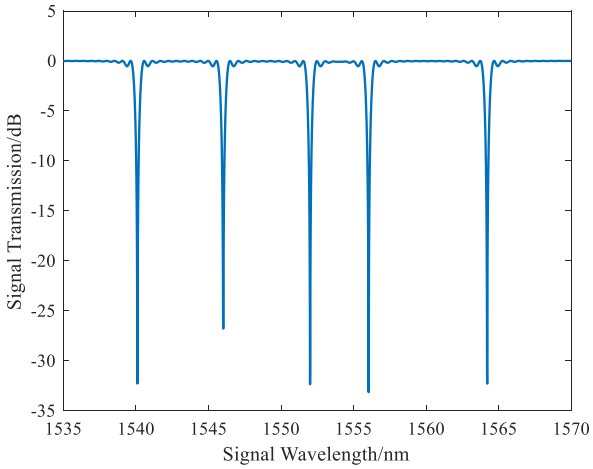

Fig. 6. Output signal transmission spectrum after change the input signal power of the fourth channel and the pump wavelength of the second channel from the ER equalized state.

new filtering channels are formed at the central wavelengths of 1564 nm and 1540 nm in the output signal spectrum, respectively. Therefore, the proposed filter is reconfigured to a five-channel bandstop filter, as displayed in Fig. 4. The corresponding ERs of the two new channels are 28.36 dB and 31.96 dB, respectively. The signal conversion efficiency at 1564 nm is 99.85%, and the signal conversion efficiency at 1540 nm is 99.94%. The bandwidths of them are all 0.43 nm.

Quite obvious ER differences can be observed among these five filtering channels. According to the analysis of the single channel filter using SFG effect in PPLN waveguide, the ER of output signal will vary following input pump power [16]. Therefore, in this multi-wavelength bandstop optical filter, the ERs of all the bandstop channels can be hopefully equalized by carefully adjusting the pump powers coupled into this filter. The equalized result of above five-channel filter is illustrated in Fig. 5. The input pump powers are adjusted to 66.34 mW, 65.95 mW, 65.90 mW, 65.51 mW and 65.08 mW, respectively. In this way, the ERs of the output filtering channels are equalized to 32.31 dB, 32.35 dB, 32.33 dB, 32.33 dB and 32.30 dB, respectively, as illustrated in Fig. 5. The ER differences are controlled within 0.05 dB after the ERs equalization. The conversion efficiencies after equalization are all about 99.94%.

However, if we change the input signal power or pump wavelength (consequently the filtering wavelength) of a channel, the equalization of ERs will be broken again, as denoted in Fig. 6. The input signal power of the fourth channel is increased to 5 mW and pump wavelength of the second channel is changed to 1544 nm. Then the corresponding signal wavelength is varied to 1556 nm. As such, the obtained ERs of the five channels are 32.31 dB, 33.14 dB, 32.33 dB, 26.77 dB and 32.30 dB, respectively. Among them, the output signal ERs of the second channel and fourth channel changed following the input pump wavelength and input signal power respectively, while the output signal ERs of other channels are fixed at the equalized value. The tolerance of the signal and pump wavelengths is very little in the SFG process. When the wavelength of signal or pump is detuned, the phase mismatch increases quickly. Therefore, the QPM condition of Eqs. (1) and (2) cannot meet between pump and pump, signal and signal, and pump and signal from different channels. That means the SFG process in each filtering channel is independent. There is no interference between different

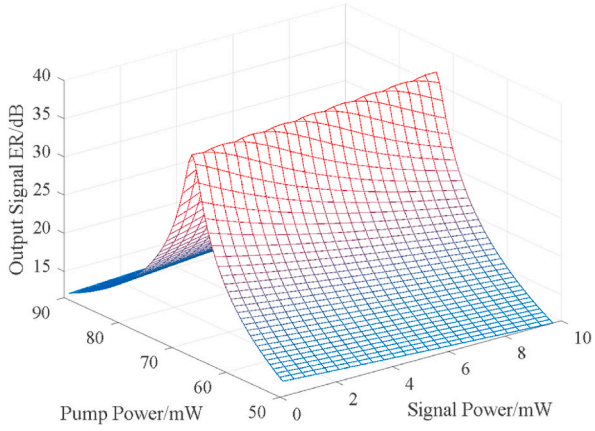

Fig. 7. The output signal ER relying on the input signal and pump powers.

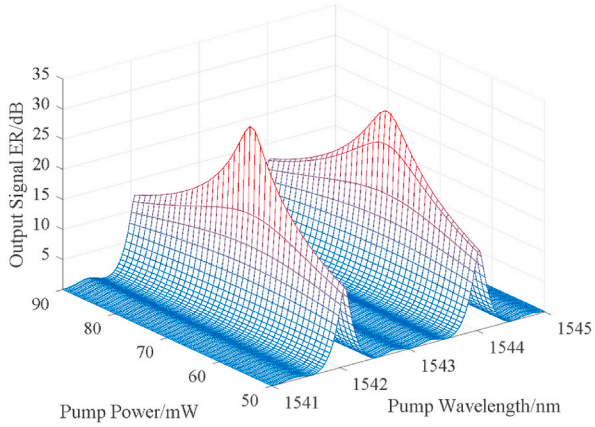

Fig. 8. The output signal ERs depending on the input pump wavelength and pump power.

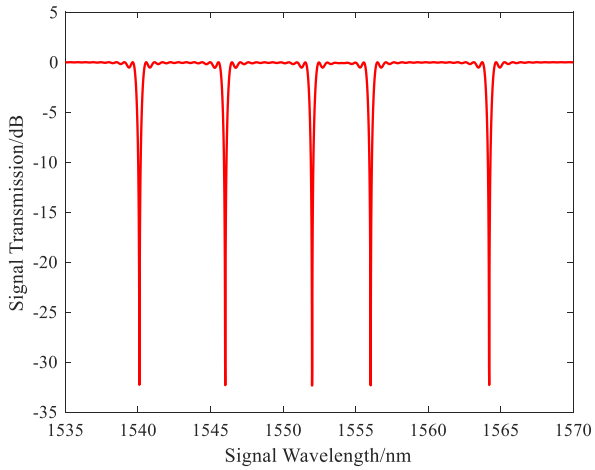

Fig. 9. The re-equalized output signal ER after the change of input signal power in the fourth channel and pump wavelength in the second channel.

channels. When the input pump wavelength of the second channel and the input signal power of the fourth channel are varied, the output signal ERs in the corresponding channels will change, but the ERs of the other channels will not change. The signal conversion efficiencies of the second channel and the fourth channel become 99.95% and 99.79%, respectively. The bandwidth of the fourth

channel varies to 0.41 nm. The bandwidth change is very little. The bandwidth of the other channels was still around 0.43 nm. This is consistent with the single channel application [16].

In order to further reveal the variation trend of the output signal ER and the equalization approach, a 3-D plot of output signal ER relying on the input signal and pump powers in the fourth channel is shown in Fig. 7. When the input signal power increase from 0.1 mW to 10 mW but the input pump power is fixed at a certain value between 50 mW and 68 mW, the output signal ER will decrease. For example, the pump power is fixed at 65 mW. When the signal power increases from 0.1 mW to 10 mW, the corresponding ER will change from 32.14 dB to 22.07 dB. Then, if we adjust the input pump power properly, the output signal ER degradation can be compensated to some extent.

Another 3-D plot of output signal ER depending on the pump wavelength and input pump power in the second channel is displayed in Fig. 8. When the pump wavelength is changed from 1541 nm to 1545 nm with the corresponding signal wavelength being tuned from 1559 nm to 1555 nm, the output signal ER will also vary. If the input pump power is adjusted properly, the output signal ER variation can be compensated to some extent.

From Fig. 6, we can find that, when the input signal power in the fourth channel increases to 5 mW, the output signal ER decreases to 26.77 dB. According to Fig. 7, the input pump power in this channel should be adjusted to 67.50 mW, then the output signal ER is compensated to 32.35 dB. The change of pump wavelength in the second channel from 1542 to 1544 nm, the corresponding filtering wavelength from 1558 nm to 1556 nm, results in the output signal ER increasing to 33.14 dB. The input pump power in this channel needs to be adjusted to 65.75 mW to obtain a little ER degeneration to 32.27 dB. In this way, the proposed multi-channel filter achieves equalization on output signal ERs again, as exhibited in Fig. 9. After re-equalization, the signal conversion efficiencies of the second channel and the fourth channel return back to 99.94%.

4. Conclusion

In this paper, we proposed and simulated a multi-channel bandstop filter by employing multi-channel SFG processes in a waveguide of PPLN. The proposed filter achieves channels number reconfigurable by setting the number of pump lights coupled into the waveguide. The central filtering wavelength of each filtering channel is tuned independently by varying the corresponding pump wavelength. The ERs of all the channels are equalized by adjusting the input pump powers. When the central wavelength or input signal power of a certain channel is changed, the ERs can be re-equalized by carefully selecting the pump power values in all the channels. Our proposed multi-channel filter has great potential applications in DWDM system, multi-point fiber sensing system and multi-channel microwave photonic filtering. If we want to realize tens/hundreds of channels, the power consumption will be a serious issue. However, lithium niobate thin film platform technology has developed rapidly. If lithium niobate thin film is used to build the proposed multi-channel bandstop filter instead of the bulk material, the power consumption of the filter can be greatly reduced and the device length can be further reduced [17,18]. This makes it easier to be integrated on an optical chip in small size.

Author contribution statement

Yuzhe Sun: Performed the experiments; Analyzed and interpreted the data; Contributed reagents, materials, analysis tools or data; Wrote the paper. Zhefeng Hu: Conceived and designed the experiments; Analyzed and interpreted the data; Wrote the paper. Shuting Cheng: Performed the experiments. Yachao Zhao; Lingfang Wang; Kaixin Chen; Wenbao Sun: Contributed reagents, materials, analysis tools or data.

Data availability statement

Data included in article/supp. material/referenced in article.

Declaration of interest's statement

The authors declare that they have no known competing financial interests or personal relationships that could have appeared to influence the work reported in this paper.

Funding statement

This work was supported in part by the National Natural Science Foundation of China No. 61501088, 62075027 and U20A20165, by the Open Project Program of Wuhan National Laboratory of Optoelectronics No. 2019WNLOKF001, by the Fundamental Research Funds for the Central Universities No. ZYGX2016J003, ZYGX2019J050 and ZYGX2020ZB015, by the Key R&D Program of Sichuan Province No. 2020YFSY0003 and by Sichuan Science and Technology Program No. 2023NSFSC0453.

References

[1] Z. Ren, Y. Sun, J. Hu, S. Zhang, Z. Lin, X. Zhi, Electro-optic filter based on guided-mode resonance for optical communication, Electron. Lett. 54 (2018) 1340–1342.

[2] B. Vidal, V. Polo, J.L. Corral, J. Martí, Photonic microwave filter with negative coefficients based on WDM techniques, IEEE Photon. Technol. Lett. 16 (2004) 2123–2125.
[3] L.R. Chen, P. Moslemi, Z. Wang, M. Ma, R. Adams, Integrated microwave photonics for spectral analysis, waveform generation, and filtering, IEEE Photon. Technol. Lett. 30 (2018) 1838–1841.
[4] A. Gautam, A. Kumar, R.R. Singh, V. Priye, Optical sensing and monitoring architecture for pipelines using optical heterodyning and FBG filter, Optik 127 (2016) 9161–9166.
[5] H. Kim, M. Yu, High-speed optical sensor interrogator with a silicon-ring-resonator-based thermally tunable filter, Opt Lett. 42 (2017) 1305.
[6] K. Chen, B. Sun, F. Chen, Z. Hu, Y. Cao, Lithium niobate photonic sensor for measurement of pulsed electric field with nanosecond risetime, Microw. Opt. Technol. Lett. 54 (2012) 421–423.
[7] B. Sun, F. Chen, K. Chen, Z. Hu, Y. Cao, Integrated optical electric field sensor from 10 kHz to 18 GHz, IEEE Photon. Technol. Lett. 24 (2012) 1106–1108.
[8] B. Sun, Z. Hu, K. Chen, F. Chen, Y. Cao, Integrated optical electric field probe for nanosecond pulse measurement, in: Photonics and Optoelectronics Meetings (POEM) 2011: Optoelectronic Sensing and Imaging vol. 8332, SPIE, 2011, p. 833206.
[9] M. Wang, J. Li, K. Chen, Z. Hu, Thin-film lithium niobate electro-optic modulator on a D-shaped fiber, Opt. Express 28 (2020), 21464.
[10] E.L. Wooten, K.M. Kissa, A. Yi-Yan, E.J. Murphy, D.A. Lafaw, P.F. Hallemeier, D. Maack, D.v. Attanasio, D.J. Fritz, G.J. McBrien, D.E. Bossi, Review of lithium niobate modulators for fiber-optic communications systems, IEEE J. Sel. Top. Quant. Electron. 6 (2000) 69–82.
[11] P.O. Weigel, J. Zhao, K. Fang, H. Al-Rubaye, D. Trotter, D. Hood, J. Mudrick, C. Dallo, A.T. Pomerene, A.L. Starbuck, C.T. DeRose, A.L. Lentine, G. Rebeiz, S. Mookherjea, Bonded thin film lithium niobate modulator on a silicon photonics platform exceeding 100 GHz 3-dB electrical modulation bandwidth, Opt Express 26 (2018), 23728.
[12] J. Wang, J. Sun, Q. Sun, W. Zhang, Z. Hu, X. Zhang, D. Huang, Experimental realization of 40 Gbit/s single-to-single and single-to-dual channel wavelength conversions in LiNbO3 waveguides with two-pump configuration, Front. Optoelectron. China 1 (2008) 3–13.
[13] J. Wang, J. Sun, W. Zhang, Z. Hu, Simulation of 40 Gbit/s NRZ to RZ format conversion based on sum-frequency generation using a PPLN loop mirror, Front. Optoelectron. China 2 (2009) 9–14.
[14] J. Wang, Q. Sun, J. Sun, Z. Hu, PPLN-based all-optical 40 Gbit/s ODB/AMI/FSK wavelength conversion and FSK logic NOT gate, Appl. Phys. B 96 (2009) 135–139.
[15] H. Liu, Z. Hu, F. Chen, J. Zhang, All-optical tunable notch filter based on SFG in PPLN waveguide, Information Optoelectronics, Nanofabrication and Testing, Optica Publishing Group, 2012.
[16] Z. Hu, M. Hou, H. Liu, F. Chen, Investigation of all-optical tunable notch filter based on sum-frequency generation in a PPLN waveguide, IEEE Photon. J. 7 (2015) 1–7.
[17] X. Li, K. Chen, Z. Hu, Low-loss bent channel waveguides in lithium niobate thin film by proton exchange and dry etching, Opt. Mater. Express 8 (2018) 1322.
[18] X. Yu, M. Wang, J. Li, J. Wu, Z. Hu, K. Chen, Study on the single-mode condition for x-cut LNOI rib waveguides based on leakage losses, Opt. Express 30 (2022) 6556.